

OTFT Technologies for Flexible Displays

Chung-Kun Song*, **Gi-Seong Ryu**, **Myung-Won Lee**, **Yong-Xian Xu**
 Dept. of Electronics Eng., media **device** lab, Dong-A Univ., Busan, Korea
 Phone: 051-200-7711, E-mail: cksong@dau.ac.kr.

Keywords : flexible display, OTFTs, AMOLED, EPD, integrated circuits

Abstract

The OTFT technologies have been mature almost up to the level of commercialization. In this paper we report the OTFT's applications to the backplane for active matrix electrophoretic, active matrix OLED and to integrated circuits. In addition we also introduce the recently developed technologies for reduction of OTFT's operating voltage.

1. Introduction

Recently, the OTFT technologies have been well developed to demonstrate active matrix electrophoretic (AMEPD) panel using OTFT-backplane [1]. Such advancement is expected to activate the development of OTFT commercialization technologies.

In this paper we report the recent results of OTFT's applications to Flexible AMEPD, active matrix OLED (AMOLED) panels and integrated circuits.

2. Experimental Procedures

We fabricated AMEPD and AMOLED panel based on OTFT-backplane. And some integrated circuits were also fabricated by using OTFTs.

The AMEPD panel consisted of 128 x 96 pixels in which each pixel was composed of OTFT and EPD. We used PEN plastic as substrate on which OTFT arrays were fabricated with Al for gate electrode and PVP for gate dielectric and pentacene for semiconductor and Au for source and drain electrodes. The critical process is deposition of interlayer between OTFT-backplane and EPD panel. The interlayer should be unharmed on OTFTs and also thick enough to prevent the effect of voltage applied to source and gate electrodes from influencing EPD panel. In addition the interlayer should be patterned to open via holes for drain electrodes to connect OTFTs to EPD without damage on OTFT-backplane.

The AMOLED panel consisted of 16 x 16 pixels in which each pixel was composed of two OTFTs and a capacitor and OLED. It was the most important to reduce the leakage current through PVP interlayer cross-over between two interconnection metal lines because a relatively large leakage current through a single cross-over make the capacitors fails to accumulate charges for driving-OTFTs. We optimized the PVP interlayer process by finding out the proper mixed ratio of components and the thickness.

The integrated circuits such as inverters, NAND/NOR gates, rectifiers, and ring oscillators based on OTFTs. We used the same processes as the above flexible displays.

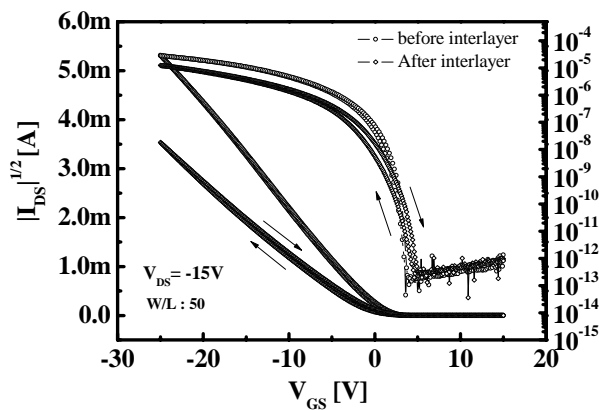
3. Results and discussion

AMEPD

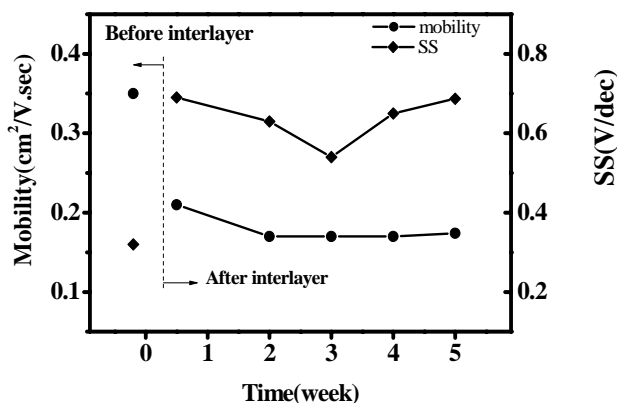
The size of backplane was 2.5" in diagonal direction and consisted of 128 x 96 pixels, containing one OTFT in each pixel. The backplanes were batch-processed on 200 mm x 200 mm PEN substrate which included four backplanes. The OTFTs employed bottom contact structure and used the cross-linked polyvinylphenol for gate insulator, pentacene for active layer. The OTFT produced good uniformity over the whole substrate area with the variation less than 20% as shown in Table 1. The OTFTs exhibited mobility of $0.21 \pm 0.02 \text{ cm}^2/\text{V}\cdot\text{sec}$, off state current $0.056 \pm 0.014 \text{ pA}/\mu\text{m}$, threshold voltage $7.42 \pm 0.59 \text{ V}$, and the Ion/Ioff current ratio of $4.8 \pm 1.36 \times 10^5$ after interlayer passivation. The interlayer degraded mobility by about 40% as shown in Fig.1a) but the degraded performance was stable even after a month operation as shown in Fig.1b). Thus, the interlayer seemed to work as a good encapsulation layer. The OTFT-EPD panel worked successfully and demonstrated to display some patterns.

Table 1. The performance parameters of OTFTs in backplane before and after interlayer deposition.

	Uniformity	After interlayer (before interlayer)
Mobility ($\text{cm}^2/\text{V}\cdot\text{s}$)	0.213 ± 0.021	0.21 (0.35)
SS(V/dec)	2.43 ± 0.43	0.69 (0.32)
Ion/Ioff	$4.8 \pm 1.36 \times 10^5$	$3.66 (14.5) \times 10^7$
Vth(V)	7.42 ± 0.59	-3.7 (-0.5)
Off-state current (pA/ μm)	0.056 ± 0.0142	0.0003 (0.0002)



(a)



(b)

Figure 1. a) The transfer characteristics of OTFT before and after PVA/Acryl interlayer deposition, and b) the variation of mobility according to time.

AMOLED

The OTFT produced the field effect mobility of $0.34 \pm 0.018 \text{ cm}^2/\text{V}\cdot\text{sec}$, off state current $\sim 10^{-11} \text{ A}$, threshold voltage $|2.68| \pm 0.35 \text{ V}$ and on/off current ratio $\sim 10^5$. The performance of printed OTFT (Ag-paste) is comparable to those of vacuum deposited OTFT (Au-thin film). The leakage current between interconnection metals was drastically reduced by optimizing the PVP-copolymer compositions and also using double layers. Thus, the capacitors were successfully charged over the threshold voltage of driving OTFTs, providing sufficient current to OLEDs to generate light. The oxygen plasma process shifted threshold voltage to the positive voltage region. Thus, the data voltage applied to the source electrode should be more positive to completely turn off the switching OTFT in order to keep the charges on capacitor be stored during scanning time. Such threshold voltage shift makes the driving scheme complicate.

In Fig.2, the final OTFT-OLED display panel with an array of 16×16 pixels and an enlarged view of the pixels is shown. The OTFT-OLED display panel generated green light as shown in Fig. 2.

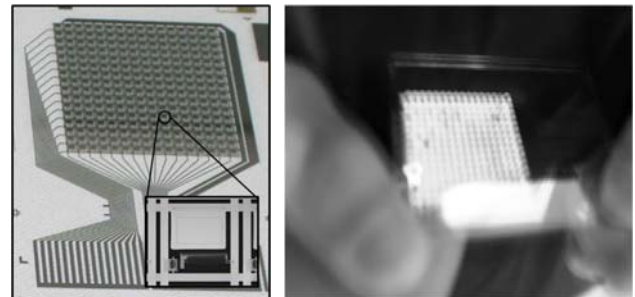


Figure 2. The AMOLED panel and its light illumination.

Integrated Circuits

The organic integrated circuits were fabricated on $200 \mu\text{m}$ thick and $5 \text{ cm} \times 5 \text{ cm}$ sized PEN substrate as shown in Fig.3. The OTFTs employed bottom contact structure and used PVP for gate dielectrics and pentacene for active layer and Al for gate electrode and Au for S/D electrodes. For interconnection the PVP gate dielectric layer was etched by oxygen plasma.

All devices and circuits were characterized in ambient air. The OTFTs produced the average mobility of $0.26 \text{ cm}^2/\text{V}\cdot\text{sec}$, on/off current ratio of 10^5 . The inverter has sufficiently large gain of about 15 as shown in Fig.4. The rectifier based on diode-

connected-OTFT generated 4V DC output voltage while input 10V AC signal at 1MHz as shown in Fig.5. The NAND and NOR gates also successfully worked at the operating voltage of 5V. The 5-stage ring oscillator produced 1 MHz oscillation frequency as shown in Fig.6, corresponding to the single stage propagation delay as low as 0.1 μ sec.

The threshold voltage shift due to the oxygen plasma process, which was used to open via holes for interconnection between drain and gate electrodes, degraded performance of inverters.

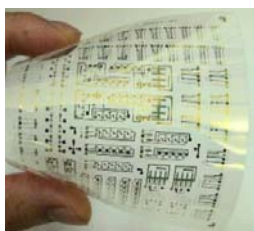


Figure 3. Photograph of plastic organic circuits

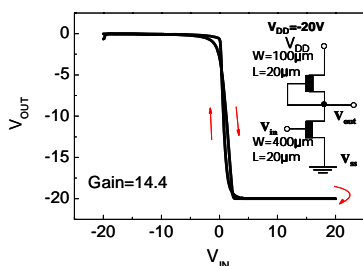


Figure 4. The transfer characteristics of inverter

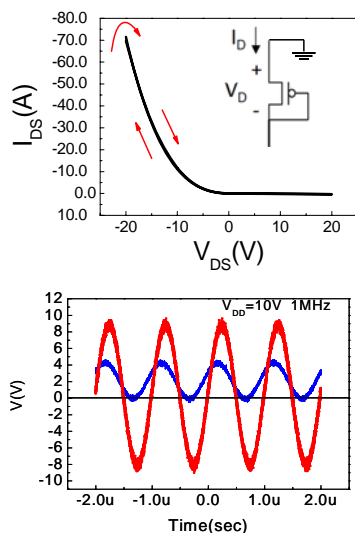


Figure 5. The diode-connected-OTFT circuit and the characteristics of rectifier

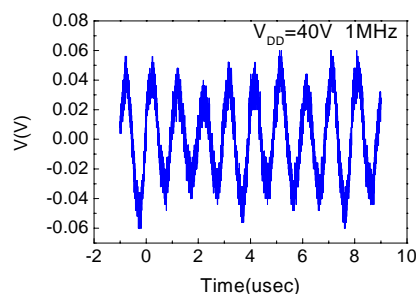


Figure 6. The output signal of 5-stage ring oscillator.

4. Summary

We fabricated AMEPD, AMOLED, and some integrated circuits based on OTFTs. The performance of OTFTs was sufficient to operate EPD. However, for AMOLED, the performance was seriously degraded after completion of fabrication so that we need to reduce the process steps. Especially, the oxygen plasma process should be replaced by another etching process to prevent threshold voltage shift.

Acknowledgements

This research was supported by a grant(F004061) from the Information Display R&D Center, one of the 21st Century Frontier R&D Program funded by the Ministry of Commerce, Industry and Energy of the Korean Government.

5. References

- [1] S.E. Burns, H. Sirringhaus, et al, SID symposium digest p.74-76 (2006).
- [2] L.Zhou, et al, *IEEE Electron Device Letters* **26** (2005) 640.
- [3] Y.Y.Choi, S.S.Yoon, J.H.Choi, H.J.Kim, J.H.Son, S.Y.Kim, Y.H.Lee, Y.H.Choi and S.T.Kim, *SID Technical Digest* (2006) 112.
- [4] M.C.Suh, J.H.Jeong, T.Ahn, J.S.Park, S.Y.Kim, Y.J.Kim, T.J.Kim, H.J.Lee, S.M.Lee, Y.W.Park, Y.G.Mo, H.K.Chung, B.W.Koo, S.Y.Kim, S.Y.Lee, *SID Technical Digest* (2006) 116.
- [5] S.Y.Lee, B.W.Koo, E.J.Jeong, E.K.Lee, S.Y.Kim, J.W.Kim, H.E.Lee, I.W.Ko, Y.G.Lee, Y.T.Chun, T.S.Oh, S.K.Kang, L.S.Pr, J.M.Kim, *SID Technical Digest* (2006) 244.